

QATAR UNIVERSITY

COLLEGE OF ARTS AND SCIENCES

THE INFLUENCE OF CARBON NANOTUBES ON THE THERMOELECTRIC
PROPERTIES OF BISMUTH TELLURIDE

By

HIMYAN MOHAMMED AKBAR

A project submitted to

the College of Arts and Sciences

in Partial Fulfillment of the Requirements for the Degree of

Master in Material Science and Technology

June 2020

© 2020 Himyan Akbar. All Rights Reserved.

COMMITTEE PAGE

The members of the Committee approve the project of
Himyan Akbar defended on 10/05/2020.

Dr. Khaled Youssef
Thesis Supervisor

Dr. Aboubakr Abdullah
Committee Member

Approved:

Ibrahim AlKaabi, Dean, College of Arts and Sciences

ABSTRACT

Akbar, Himyan, M., Master:

June: 2020, Master of Material Science and Technology

Title: The Influence of Carbon Nanotubes on the Thermoelectric Properties of Bismuth Telluride

Supervisor: Dr. Khaled Youssef

Thermoelectric materials are devices that have the ability to convert waste heat to electricity. The widespread use of thermoelectric materials is currently limited by the low value of their figure-of-merit (ZT). Bismuth Telluride (Bi_2Te_3) is a promising thermoelectric material in the near room temperature applications that provides a ZT value ~ 1 . In order to overcome the limitation of utilizing thermoelectric materials in waste heat recovery, a ZT value > 2 is required. In this current study, multi-walled carbon nanotubes (MWCNT) were incorporated into the Bi_2Te_3 bulk matrix system to enhance its mechanical and thermoelectric properties through powder processing techniques. The nanocrystalline $\text{Bi}_2\text{Te}_3/\text{MWCNT}$ composites were prepared using high energy ball milling and spark plasma sintering (SPS) techniques. The structural characterization and the average grain size values of both pristine Bi_2Te_3 and $\text{Bi}_2\text{Te}_3/\text{MWCNT}$ were found to be approximately (~ 13 nm), and the average strain was found to be 0.2 using both X-ray Diffraction (XRD) and Transmission Electron Microscopy (TEM) techniques. Vickers Microhardness test shows significant improvement of the nanocomposite hardness up to ~ 2 GPa as a function of increasing the MWCNT content. As for the dimensionless figure of merit (ZT) of the

composite, it is expected to increase above the value of the pure binary Bi_2Te_3 in the temperature range of 298–498 K the addition of MWCNT increased the ZT value from 0.48 to maximum ZT value to 0.61 at 50°C, while at 150°C the ZT value was measured to be 0.35 and 0.43 for Bi_2Te_3 and MWCNT/ Bi_2Te_3 , respectively. It is considered that the enhancement of the thermoelectric performance of the composite mostly derived from the thermal conductivity, which is reduced by an active phonon-scattering at the MWCNT/ Bi_2Te_3 interfaces.

DEDICATION

This thesis is dedicated to the one soul I lost during this journey, the one who made me start this mission of pursuing this degree. For those who stood by my side during highs and lows my older sister Huda and younger brother Faraj. For all the friendships I lost and all the friendship I gained. I believe without them, it would be impossible to reach this goal.

ACKNOWLEDGMENTS

I would like to express my sincere gratitude to Dr. Khaled Youssef; I am really fortunate and grateful that I had such a kind and patient supervisor. His excellent guidance and constant encouragement have been a great influence in my research work, course studies, and writing of this thesis made this journey possible. A special thanks to Dr. Aboubakr Abdullah for being there whenever needed.

My genuine gratitude is further extended to the faculty members of Materials Science and Technology Program at Qatar University; Dr. Ahmed Elzatahry, Dr. Talal Altahtamouni, Dr. Khaled Youssef, Dr. Aboubakr Abdullah and Dr. Igor Krupa for their teaching, lecturing, and courses which have a massive impact in improving and strengthening my knowledge and background in many areas especially this field.

Also, I would like to thank Miss Farah Elmakaty, for guiding me through the right path for characterizations whenever I needed assistance. I truly appreciate her assistance and advice throughout my research.

I would like to thank the staff at the Center for Advanced Materials (CAM) for allowing me to use some of their equipment and for conducting some tests. Central Laboratory Unit (CLU) for their assistance throughout my research period.

I would like to acknowledge the financial support of the Qatar National Research Fund (a member of Qatar Foundation) through the National Priorities Research Program NPRP10-0206-170366 Without their funding, this research would not have been possible.

Table of Contents

DEDICATION	V
ACKNOWLEDGMENTS	VI
LIST OF TABLES	IX
LIST OF FIGURES	10
CHAPTER 1: INTRODUCTION	12
CHAPTER 2: LITERATURE REVIEW	14
2.1. Thermoelectric materials and their properties.....	14
2.2. Bismuth Telluride thermoelectric material	14
2.3. Approaches to improve ZT values	16
2.3.1. Nano-structuring.....	16
2.3.2. Nano-compositing	17
CHAPTER 3: METHODOLOGY	22
3.1. Materials.....	22
3.2.1 Ball milling process	24
3.2.2 Spark plasma sintering (SPS)	26
3.3 Characterization techniques	27
3.3.1 Scanning electron microscopy (SEM)	27
3.3.2 Transmittance electron microscopy (TEM).....	28

3.3.3 X-ray diffraction (XRD).....	28
3.3.4 Vickers microhardness	29
3.3.5 Density measurements and porosity	30
3.3.6 Differential scanning calorimeter (DSC).....	30
3.3.7 Thermoelectric Properties.....	31
CHAPTER 4: RESULTS AND DISCUSSION.....	34
4.1. Surface morphology and composition.....	34
4.1.1. Scanning electron microscopy (SEM) and Energy dispersive X-ray (EDX) ..	34
4.1.2. X-ray diffraction (XRD).....	36
4.1.3. Transmission electron microscopy (TEM).....	38
4.2. Mechanical and physical properties	40
4.2.1. Vicker microhardness	40
4.3. Thermal and electrical properties.....	43
4.3.1. Differential scanning calorimeter (DSC).....	43
4.4. Thermoelectric measurements.....	45
4.4.1 Thermoelectric properties of Bi_2Te_3 and MWCNT/ Bi_2Te_3	45
4.4.2. The figure of merit (ZT)	48
CHAPTER 5: CONCLUSION	49
CHAPTER 6: REFERENCES	50

LIST OF TABLES

Table 1: The final measurements in grams for the base material	24
Table 2: Reports all the volume fractions of the base material and the volume fraction of CNT.....	25
Table 3: Shows the DSC experimental conditions	32
Table 4: Shows the grain size and the strain of Bi_2Te_3 and the dropped MWCNT/ Bi_2Te_3	39
Table 5: Shows the microhardness values (H_v) based on the MWCNT content.....	43
Table 6: Shows the microhardness values (H_v , MPa and GPa) based on the MWCNT content.....	43
Table 7: Shows the DSC results of the base on doped Bi_2Te_3 with MWCNT	45

LIST OF FIGURES

Figure1: The rhombohedral unit cell of bismuth telluride.....	16
Figure 2: The density of CNTs versus the outer diameter for different number of walls..	22
Figure 3: Schematic diagram represents the mixing process of Bi ₂ Te ₃ /SWCNT nanocomposite by ball milling method; (a) Bi ₂ Te ₃ , (b) MWCNT, (c) Bi ₂ Te ₃ /MWCNT after mixing.	27
Figure 4: Show the schematic of Spark Plasma Sintering (SPS) of Bi ₂ Te ₃ /MWCNT.....	28
Figure 5: shows the MWCNT used to dope Bi ₂ Te ₃ base.....	36
Figure 6: SEM images shows the composites alloys a) Bi ₂ Te ₃ , b) 1% MWCNT/Bi ₂ Te ₃ ..	36
Figure 7: Shows the EDX analysis of the composites alloys a) Bi ₂ Te ₃ , b) 1% MWCNT/Bi ₂ Te ₃	37
Figure 8: XRD analysis of as prepared Bi ₂ Te ₃ , Bi ₂ Te ₃ –0.05% MWCN, Bi ₂ Te ₃ – 0.1% MWCNT, Bi ₂ Te ₃ – 0.25% MWCNT, Bi ₂ Te ₃ – 0.5% MWCNT and Bi ₂ Te ₃ – 1%MWCNT.....	38
Figure 9: Shows the liner fit of Averbach method to calculate the Grain size and Lattice strain of Bi ₂ Te ₃ as function of different MWCNT content.....	39
Figure 10: shows a) bright-field TEM image, b) dark-field TEM image of MWCNT-Bi ₂ Te ₃	40
Figure 11: Shows the Grain size distribution of MWCNT-Bi ₂ T ₃ and the Lorentz fitting of the fraction distribution.....	41

Figure 12: Shows the microhardness values (GPa) based on the MWCNT content.....44

Figure 13: DSC curve of the 1st heat analysis of bismuth telluride and the doped alloy..45

Figure 14: DSC curve of the 2nd heat analysis of bismuth telluride and the doped alloy.46

Figure 15: Shows the Bi_2Te_3 and $\text{MWCNT}/\text{Bi}_2\text{Te}_3$ prepared by ball milling and SPS.
a)Electrical conductivity, b)Seebeck Coefficient, c)Thermalconductivity and d)Power
Factor.....48

Figure 16: Comparison between the figure of merit (ZT) of Bi_2Te_3 and $\text{MWCNT}/\text{Bi}_2\text{Te}_3$
nanocomposite.....49

CHAPTER 1: INTRODUCTION

Thermoelectric materials are materials that have the ability to convert the thermal energy into electrical energy or vice versa (J.Sharp, 2006). They are known as energy converters, by converting waste heat to electricity or by cooling down the hot parts of the devices (F.J. Disalro, 1999). Thermoelectric materials and its devices are becoming further prominent as power generators devices that convert waste heat into electrical energy. The need to obtain and develop high-efficiency thermoelectric materials is vital in order to provide alternative energy devices and technologies to reduce the global dependence on fossil fuels as well as to reduce greenhouse emissions. Therefore, it is essential to develop thermoelectric materials for managing waste/heat recovery and carry enormous economic and environmental benefits.

The Seebeck effect, or what known as the thermopower, is when a temperature difference take place through the material inducing the electrical potential difference that is proportional to the temperature difference that took place (Tritt and Subramanian, 2006). This effect is used in power-generation devices. The ratio of the voltage difference to the temperature difference is called the Seebeck coefficient and is an intrinsic property of the material. The efficiency of energy conversion of the thermoelectric materials depends on the figure of merit (ZT) Equation 1:

$$ZT = \frac{S^2 \sigma T}{\kappa} \quad (1)$$

Where (S) is the Seebeck coefficient, (σ) is the electrical conductivity, (T) temperature in kelvin, and (κ) is the thermal conductivity. The resulted product of ($S^2\sigma$) is known as the

power factor (PF) of the thermoelectric material. Increasing the power factor leads to enhancement in the thermoelectric properties of the material, whereas the value of ZT can be controlled by changing the Seebeck coefficient, either by using a combination of high electrical conductivity and low thermal conductivity or low electrical conductivity and high thermal conductivity.

The main objective of this research work is to enhance the thermoelectric properties of Bi_2Te_3 using both nanostructuring and nano-compositing techniques with MWCNT. In this current study, MWCNT was incorporated into Bi_2Te_3 bulk materials matrix system based on molecular level mixing to enhance its mechanical and thermoelectric properties through the powder processing technique as a function of temperature. The nanocrystalline CNT/ Bi_2Te_3 composites were successfully prepared using high energy ball milling and Spark Plasma Sintering (SPS) techniques. The structural characterization and the average grain size of both pristine Bi_2Te_3 and CNT/ Bi_2Te_3 were investigated using both X-ray Diffraction (XRD) and Transmission Electron Microscopy (TEM) analysis techniques. Vicker microhardness test and diffraction scanning calorimeter were used to study the mechanical properties, and thermal properties of Bi_2Te_3 as the amount of MWCNT was increased. Seebeck coefficient and electrical conductivity were both measured simultaneously in the SBA 458 Nemesis system, at different temperatures. To determine thermal conductivity, Light Flash Apparatus LFA 467 HyperFlash was used. The results obtained showed the success of MWCNT/ Bi_2Te_3 fabrication of nanostructured composite with enhanced thermoelectric performance and high Seebeck coefficient.

CHAPTER 2: LITERATURE REVIEW

2.1. Thermoelectric materials and their properties

Thermoelectric materials (TE) are materials that exhibit the Seebeck and Peltier effect. They possess a narrow energy bandgap, which labels them in the category of the semiconductors. Their energy band gap is usually less than 0.25 eV at a temperature of 300 K (Tritt and Subramanian, 2006). In the case of thermoelectric device manufacturing, a collection of thermoelectric couples are used. A thermoelectric couple involves a *p*-type and an *n*-type semiconductor sandwiching an electrical metallic pad (Tritt and Subramanian, 2006). Throughout history, many scientists and researchers have studied the properties of thermoelectric material in order to improve their ZT values. The main founder of the research is thermoelectric performance can be controlled by the crystal structure, grain size, and orientation. In the 1960s, scientists had focused on doping systems such as $\text{Bi}_2\text{Te}_3\text{-Sb}_2\text{Te}_3$ and PbTe-SnTe as a method to enhance their thermoelectric properties. Through doping, scientists aimed to introduce more defects into the alloy system that enable phonons scattering and reducing the lattice thermal conductivity (C. Gayner and K. K. Kar, 2016).

2.2. Bismuth Telluride thermoelectric material

Bismuth telluride is a semiconductor material with a small energy gap that equals to ~ 0.11 eV. It is one of the most used thermoelectric materials due to its near room temperature applications. Its ability to convert heat energy into electrical energy is very desirable. The crystal structure of Bismuth telluride is a crystal rhombohedral structure. A structure category consist of five atoms arranged in layers on top of each other in order of

Te-Bi-Te-Bi-Te, it can be considered as a layered semiconductor material Figure 1. Bi_2Te_3 layers consist of bismuth (Bi) and Tellurium (Te) atoms, Where both atoms are tightly packed along the C-axis, which also known as quintuple layers. The bonding between Bi and Te atoms in one layer are ionic or covalent bonding, which are considered one of the strongest bonds. However, the bonds between each layer are weak van der waal type of bond. The lattice parameters and the energy band gap (E_g) of Bi_2Te_3 are reported as follow; $a/\text{\AA}$ (4.38), $c/\text{\AA}$ (30.48), unit layer/ \AA (10.16) and E_g/eV (0.15).

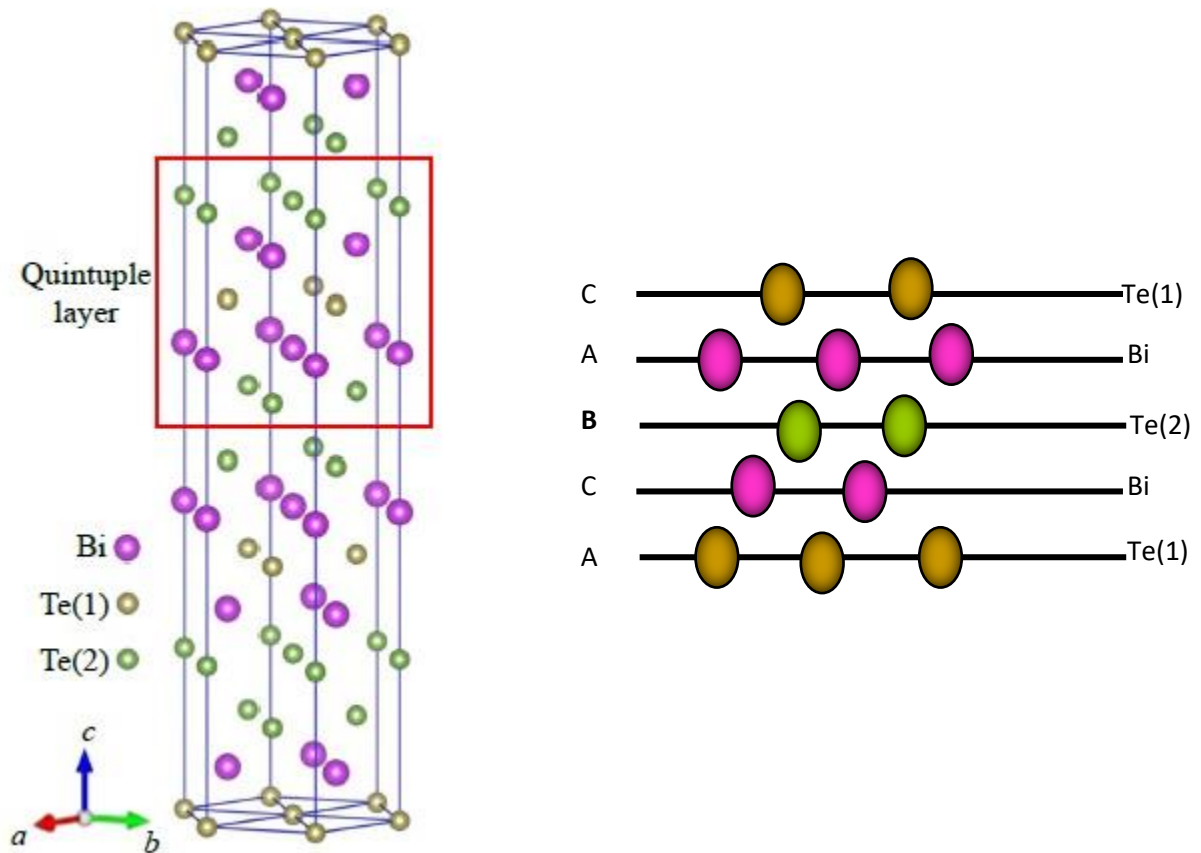


Figure 1. The rhombohedral unit cell of bismuth telluride.

In the late years, more than a dozen studies have been conducted to acquire high-efficiency thermoelectric materials via the development of Bi_2Te_3 nanostructure. One study done by Ramanath et al. (G. Ramanath, 2012) proposed that the porous nanoscale material can aid significantly in increasing the ZT value of n-type Bi_2Te_3 doped with sulfur. Nevertheless, the lifetime of these materials is short, due to their unstable structure that results in grain growth.

2.3. Approaches to improve ZT values

Materials with relatively high ZT potential require a large Seebeck coefficient (S), which can be found in low electrons concentration carrier semiconductors or insulators, and a high electrical conductivity such as metals. Hence, the thermoelectric power factor should range between the concentrations carrier of semiconductors and metals.

Two approaches are used to enhance the thermoelectric properties, especially the ZT value; (1) nanostructuring, and (2) compositing. It was also found that these nanostructures can improve the Seebeck coefficient (W. Kim, NA).

2.3.1. Nano-structuring

The nanostructuring techniques, which is an intrinsic method, increase the phonon scattering at the grain boundaries over a large scale of free path while preserving the value of the mobile carries and lower the thermal lattice conductivity (Xie W, 2009). Nano-structuring can improve the density of states (DOS) of the electrons in the semiconductor materials near the Fermi level, therefore increasing the thermopower. Nano-structuring introduces large density interfaces materials in which enable phonons to be scattered more efficiently and better than electrons and reducing the thermal conductivity power factor of

the lattice while preserving the carrier's mobility and the electronic conduction. Several synthesis techniques were used to fabricate materials that can be controlled at the nanoscale. One of the most used methods to control the size of the materials at the nanoscale is ball milling (C. Gayner and K. K. Kar, 2016). Ball milling is a mechanical technique used to mix two or more powder materials to form nanoparticle size alloys. The size reduction is taking place due to different size stainless steel, tungsten carbides, or zirconia balls. The milling process takes place under an inert gas, usually argon to prevent any oxidation. The high speed and ball to powder ration cause the release of high energy during the collision resulting in size reduction (C. Gayner and K. K. Kar, 2016).

2.3.2. Nano-compositing

The compositing technique is a promising method to enhance the thermoelectric properties, which consist of matrix or base material and a nanosized dispersoid. The nano compositing method aims to reduce the thermal conductivity with minimal effect on the electrical conductivity due to the newly formed interface between the matrix and the nano dispersoid at the grain boundaries. The nano-dispersoid or nano-precipitates act as carriers with minimal kinetic energies that can be interrupted or stopped very easily by the energy barrier at grain boundaries and allow electrons with high energy to pass through effortlessly (Z. G. Chen & others, 2012).

2.3.2.1. Type of fillers in nano-compositing

Nano-fillers are considered to be materials that are anticipated to improve the thermoelectric properties of the alloy. It can be classified as 1D, 2D, and zero D materials. The filler size, shapes, amount, the way it distributed, and orientation inside the matrix can affect the thermoelectric properties of the alloy. Zero dimension filler known as quantum dots, 2D filler as quantum wire, and 1D as quantum wire depending on their dimensions at the nanoscale. The most used 2D fillers are graphene sheets and graphene powders. Zero D fillers are silicon carbide and zirconium oxide, as for 1D filler is multi or single carbon nanotubes (MWCNT/SWCNT) are the most used.

2.3.2.2. CNT as a filler in thermoelectric materials

Carbon nanotubes (CNT) are known for their exceptional mechanical, electrical, and thermal stability; it inherently displays high mobility for carrying electrons, which in turn leads to high electrical conductivity. In a study done by Kim and Zide (W. Kim, & J. Zide, NA) the thermoelectric properties of Bi_2Te_3 system were enhanced through compositing, by adding nano gold particles as reported in Nguten and Enju's research (T. H. Nguyen, J. Enju, 2019) or by adding different filler such as graphene as D. Suh and S. Lee have done in their study (D. Suh & S. Lee, 2015). The main objective of this type of technique is to introduce some impurities and creates a new interface at the grain boundaries that increases the material ability to scatter phonons, leading to a reduction in the thermal conductivity (Q. Lognoné, & F. Gascoin, 2015). The compositing material volume, size, quantity, structure, shape, distribution, and the way its orientated can affect the base material properties. Hence, the size of the filler can play a major role in enhancing

the thermoelectric properties if controlled. The nano-size materials ($\sim < 100\text{nm}$) such as CNT tend to segregate on the grain boundaries creating a new interface. The smaller the particles, the more pathways the electrons have to travel, a mechanism that can filter out the low mobility electrons.

The dispersion of CNT in the Bi_2Te_3 system can enhance its ability to scatter phonons at the grain boundaries or at the interface due to its capability of carrying electrons. Some studies and research suggested that the distribution of CNTs or fullerene -an allotrope of carbon- have the ability to boost the interfaces and improve the microstructure leading to an enhancement in thermoelectric performance (K. T. Kim, 2013) and (N. Gothard, 2011). Therefore, adding the CNT to Bi_2Te_3 should influence the thermoelectric properties of the whole system. Optimizing the concentration of CNT in Bi_2Te_3 could result in obtaining the anticipated characteristics of the thermoelectric material.

The new approach in cultivating nanostructuring of bismuth telluride material could lead to further improvements of its ZT value. Ren and his crew of researchers have reported ZT value of Bi_2Te_3 system that equals to ~ 1 that is suitable for applied commercial applications (F. Ren, H. Wang, P.A. Menchhofer and J.O. Kiggans, 2013). Other researchers reported the introduction of non-thermoelectric materials through solid-state solution techniques. Their result concluded that the addition of such materials as C_{60} (0~1.3%) along with single-walled carbon nanotubes (0.5~5%) in Bi_2Te_3 bulk matrix system led to some enhancement in the Seebeck coefficient and reduced the thermal conductivity of the whole system (D. H. Park, M. Y. Kim and T. S. Oh, 2011). In the year 2008, a group of researchers had doped the $\text{Bi}_{0.4}\text{Sb}_{1.6}\text{Te}_3$ system with multi walled carbon

nanotubes and have found out the ZT value was unchanged, although the noticeable enhancements in the mechanical properties. Several attempts for composites fabrication using CNT took place during the past years. One of these attempts was performed by using a polymeric system. The ZT values obtained during this study were disappointing due to the nature of polymer used, in which the huge complex molecular nature of the polymer hindered the transportation of the electrons carries (C. Yu, Y. S. Kim, D. Kim and J. C. Grunlan, 2008). A small number of studies suggested the investigation of CNT/Alloys thermoelectric properties in order to have a full view of the grain boundaries and the newly formed interface due to the addition of CNT. Khasimsaheb has suggested that the addition of different weight percentage (0.025, 0.05 and 0.1%) of CNT into lead telluride (PbTe) system have the potential of enhancing the thermoelectric properties of the system, in this study it was found that the electrical conductivity and Seebeck coefficient of PbTe alloy doped with 0.05% CNT distributed in the PbTe matrix had been enhanced by the power of two of the undoped alloy above 450 K (B. Khasimsaheb, 2017). In the mentioned system (PbTe), CNT's acted as a low energy filter at the potential barrier and good passage for high energy electron, which causes the enhancement of the electrical conductivity. However, the density and weight of the CNT can play a major in affecting the thermoelectric property and the ability to carry electrons. It is reported by (K. T. Kim and others, 2013) the ZT value obtained when multi-walled-carbon nanotube (MWCNT) was used; the results reported a ZT of 0.85 at a 473 K compared to the Zt value of the binary system bismuth telluride. Whereas, in the case of single-walled carbon nanotube (SWCNT) the ZT enhancement of bulk Bi_2Te_3 alloy reached up to 25% using only 0.5 wt%. However,

depending on the SWCNT doping level and the temperature, the sign of the Seebeck coefficient was changed from n-type to p-type (Y. Zhang and others, 2012). Another study was done by (C.H. Laurent, 2010) to measure the density of CNT based on the diameter of the nanotubes. Figure 2 The density of SWCNTs and MWCNT versus the outer diameter.

Based on Figure 2, the density and number of walls of CNT can affect the ability of it electron carrier significantly. Thus, it is essential to fabricate Bi_2Te_3 with enhanced thermoelectric properties doped with MWCNT. Where the MWCNT is homogeneously dispersed in the Bi_2Te_3 system, and the ZT values will be studied thoroughly and will determine the effectiveness of MWCNT on the thermoelectric properties.

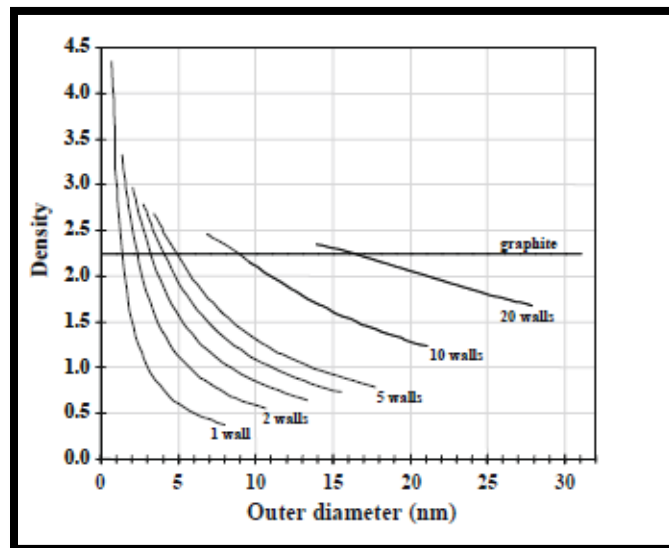


Figure 2. The density of CNTs versus the outer diameter for different number of walls.

CHAPTER 3: METHODOLOGY

This chapter is composed of two main sections. The first section describes the materials used, and the procedure for preparing the MWCNT/Bi₂Te₃ nanocomposites are introduced. In addition, the high energy ball milling technique, as well as the spark plasma sintering (SPS) and the requirements used to fabricate the samples, are explained. The next section lists the characterization methods applied to assess the structural, mechanical, thermal and thermoelectric properties of the material.

3.1. Materials

The starting materials were obtained Bismuth (Bi) metal powder (99.9% pure, 9.747 g/cm³), and Tellurium (Te) metal powder (99.99% pure, 7.74 g/cm³). The powders are used as a base material in order to introduce multi-walled carbon nanotube (MWCNT) into the alloy. Different concentrations of MWCNT were used to optimize the content (0.05, 0.1, 0.25, 0.5, and 1 Vol%) and added to the base metals at the early stages of the mixing process. The MWCNTs were synthesized through the decomposition of hydrocarbon gas in a modified microwave chemical vapor deposition (CVD) . The weighing process of the powders took place in a controlled environment chamber (mBRAUN) under an ultra-high purity Argon gas.

In order to calculate the proper amounts of the starting material, Equation 2 was used to measure the precise weight in grams (g) of bismuth, telluride, and MWCNT.

$$wt\% (x)_A \frac{AT\%(A)*(MW)_A}{AT\%(A)*(MW)_A + AT\%(B)*(MW)_B} \times 100 \quad (2)$$

Where wt.% is the weight percentage, and at.% is the atomic weight of each material, and MW is the molecular weight of the pure powders. Table.1 summarize the above equation for both bismuth and tellurium weighing measurements. The total weight of the combined materials was 7g.

Table 1. The Final Measurements in Grams for the Base Material.

Composition	Element	Molecular weight (g/mole)	Atomic weight (%)	Weight (%)	Mass (g)
Bi₂Te₃	Bi	208.98	40	52.20	3.65
	Te	127.60	60	47.80	3.35
	Total			100	7

Table.2 summarizes the final weighing measurements of MWCNT after all the calculations required are done. The different volume fraction of MWCNT was used (0.05, 0.1, 0.25, 0.5 and 1Vol%), in which the molecular weight of MWCNT used is 12.1 g/mole. Based on the below measurements in Table 2 each composition powder material was weighted and subjected to the ball milling process.

Table 2. Reports all the Volume Fractions of the Base Material and the Volume Fraction of MWCNT.

Composition	Element	AT%	Wt%	ρ (g/cm ³)	Mass (g)	V _o	V _f (%)
Bi₂Te₃-0.05%MWCNT	Bi	39.9619	52.192	9.747	3.6534	0.373	41.01
	Te	59.9429	47.801	7.74	3.3461	0.536	58.94
	MWCNT	0.0952	0.007	1.1	0.0005	0.000	0.05
	Total					7.000	0.909

Bi₂Te₃-0.1%MWCNT	Bi	39.9238	52.188	9.747	3.6532	0.373	40.99
	Te	59.8858	47.798	7.74	3.3458	0.536	58.91
	MWCNT	0.1904	0.014	1.1	0.0010	0.001	0.10
	Total				7.000	0.909	100
Bi₂Te₃-0.25%MWCNT	Bi	39.8099	52.177	9.747	3.6524	0.373	40.93
	Te	59.7148	47.787	7.74	3.3451	0.536	58.82
	MWCNT	0.4754	0.036	1.1	0.0025	0.002	0.25
	Total				7.000	0.909	100
Bi₂Te₃-0.5%MWCNT	Bi	39.6206	52.158	9.747	3.6511	0.373	40.83
	Te	59.4308	47.770	7.74	3.3439	0.536	58.67
	MWCNT	0.9486	0.072	1.9	0.0050	0.005	0.50
	Total				7.000	0.909	100
Bi₂Te₃-1%MWCNT	Bi	39.2445	52.120	9.747	3.6484	0.373	40.62
	Te	58.8668	47.736	7.74	3.3415	0.535	58.38
	MWCNT	1.8887	0.144	1.9	0.0101	0.009	1.00
	Total				7.00	0.908	100

3.2.1 Ball milling process

The prepared powders were mixed by a laboratory mechanical ball mill (SPEX SamplePrep 8000M Mixer/Mil). The collision of particles produces high power leading to severe plastic deformation in order to reduced particle size and obtain a homogeneous material. This technique is wildly used and well known for its economical and simplicity to process and obtain nanostructured materials with small particle size range in a range of (less than 100 nm). Some of the drawbacks of this technique are the possible defects and the ununiform distribution of the particle size (C. Suryanarayana,2011). The procedure

involves filling the milling container with the mixture of powders that were prepared in a stoichiometric. The process takes place under atmosphere inert gas of Argon ($O_2 < 0.5$ ppm) to ensure the proper mixing of the powders and maintain a stable phase/nanosized phase of the nano-composition. The high milling speed and the ball to powder ration cause the release of high energy during the collision that contributes to the size reduction of the powders. The collision process and the force impact of the balls and the powder trapped between them are shown in Figure 3. However, a very critical high speed would cause the balls to be paralyzed and stuck on the inner wall of the container preventing the collision and size reduction of the powders.

Different volume percentage of MWCNT (0.05, 0.1, 0.25, 0.5 and 1 vol%) were mixed in Bi_2Te_3 system Figure 3. The milling process was conducted using 7.94 mm and 6.35 mm steel balls with a Ball to Powder Ration (BPR) of 7:1, the milling balls displayed insignificant weariness. The BPR can significantly influence the milling duration, where a higher ratio and large weight permits for faster movements that cause an increase in the number of collisions/time, increasing the amount of energy transferred to the powders particles. The use of different balls sizes aids in reducing the amount of powders coating the inner walls of the container creating shearing forces that aid in removing the powder from the surface of the ball. The milling process duration was up to 16 hours under a (1725-1425) rpm and 60-50 Hz at room temperature. The mixed powders were again placed inside the control chamber for collecting purposes to prevent any oxidation or contamination due to air exposure.

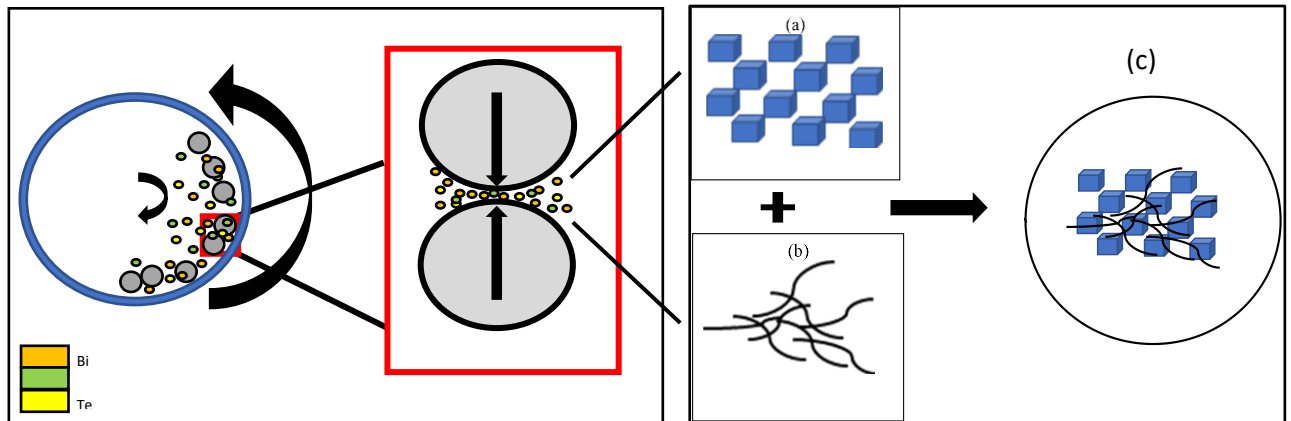


Figure 3. Schematic diagram represents the mixing process of Bi₂Te₃/MWCNT nanocomposite by ball milling method; (a) Bi₂Te₃, (b) MWCNT, (c) Bi₂Te₃/MWCNT after mixing.

3.2.2 Spark plasma sintering (SPS)

Spark plasma sintering (SPS) is a process suitable for thermoelectric materials fabrication. This technique is used to preserve the nanostructure of the material while reaching a high compaction density of the pellets since it can restrict grain growth while sintering at low temperatures and in a short time. In one study conducted by Wang et al., The fabricated thermoelectric material Pb-Ag-Te-Sb with fine grains by mechanical alloying and Spark plasma sintering exhibit high performance (L. D. Zhao, B. -P. Zhang. 2008).

Samples used in this research were sent to Texas A&M University, Materials Science and Engineering Department for SPS. Each sample weighing ~3 g was loaded into the graphite die and placed inside the SPS chamber figure 4. The whole process takes place under vacuum with a heating rate of 25°C/min. The compacted pellets are subjected to various analysis tests to investigate their properties.

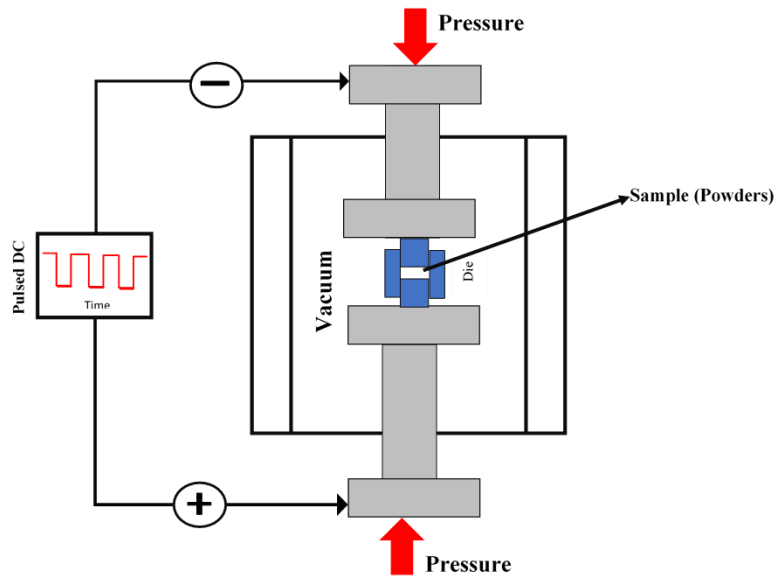


Figure 4. Show the schematic of Spark Plasma Sintering (SPS) of $\text{Bi}_2\text{Te}_3/\text{MWCNT}$.

3.3 Characterization techniques

3.3.1 Scanning electron microscopy (SEM)

Scanning electron microscopy (SEM) is one of the most used tests of investigating the surface morphology of the samples. It is considered to be one of the many microscopic used tools. SEM uses a focused electron beam to produce images of a sample surface by scanning it. The electrons from the beam interact with the atoms on the sample surface, generating the SEM image. Several signals comprise different information about the sample surface topography, and sample composition can be obtained from this test.

Scanning electron microscopy (SEM) was used to investigate the homogenous distribution of CNT particles in the Bi_2Te_3 matrix. The surface morphology and the distribution of the particles will also be assessed using SEM.

3.3.2 Transmittance electron microscopy (TEM)

Transmittance electron microscopy (TEM) is one of the analysis techniques used for imaging the samples at a very small scale than are less than 100nm in length. It can detect the structural lattice atoms position, defects, slip planes, the grain size, and their distribution. According to De Broglie principle about the wavelength; each material has the ability to absorb light in distinctive wavelength range, based on that range the interaction between the electron beam in TEM and the sample electron results in creating an image of how the atoms are behaving in that scale and how they are distributed. There are two types of TEM images, which are the dark field image and the bright field image; the concept of these images depends on the atom weights. Heavier atoms lead to high scattering and high-resolution images. TEM was utilized during this research work to conform to the grain size and validate the results acquired from XRD.

3.3.3 X-ray diffraction (XRD)

X-Ray Diffraction (XRD) considered a widely used nondestructive technique to determine the crystallinity degree of the material to identify the phases, determine the crystal structure as well as the lattice parameter measurements; such as the grain size and strain calculations. X-ray diffraction (XRD) analysis was conducted on Bi₂Te₃ alloy using PANalytical Empreon diffractometer, where the applied voltage is 45kV. The samples were exposed to Cu K_α radiation ($\lambda = 1.54056\text{\AA}$) in the scanning range 10°-90° at a scanning speed of 2 deg/min. The XRD was used to determine the crystallite/grain size and to

determine Hall–Petch contribution of MWCNT to the Bi₂Te₃ hardness, the amount of strain the system was subjected to, and the nature of severe plastic deformation (SPD) that took place during the milling process. Based on Averbach equation Equation 5, the grain size of each system was calculated from the Gaussian fit of the peaks using Origin-Pro analysis software.

$$\frac{(\delta 2\theta)^2}{\tan^2\theta} = \frac{\lambda}{d} \left(\frac{\delta 2\theta}{\tan\theta \sin\theta} \right) + 25(e^2) \quad (5)$$

Where $\delta 2\theta$ is the FWHM, θ is the diffraction angle of the peak's, λ is the X-ray wavelength of 0.154 nm, d is the grain size, and e is the strain.

3.3.4 Vickers microhardness

Vickers micro-hardness considered one of the most used nondestructive tests; it aids in evaluating the mechanical properties of a sample. The material hardness is a character associated with the material ability to withstand plastic deformation. Elements that can alter or impact the disruption movement of the grains can affect Bi₂Te₃ alloys' hardness. The alloy hardness value depends on various factors, such as the volume fraction and density of the doped or the reinforcement phases (MWCNT). The microhardness values of the pellets were measured using Vickers microhardness tester FM ARS 9000, the applied load was 25gf, and the dwell time was 10 sec, six different indentation measurements at a different position on the sample surface were made. The indented diagonal shape was measured using the microscope equipped along with the HV hardness machine.

3.3.5 Density measurements and porosity

In order to estimate the level of porosity and the relative density of Bi₂Te₃ alloy, the Archimedes principle was applied to measure the densification of Bi₂Te₃ alloy. It connects the relative density of the alloys used in reference to the used fluid in this case water. The actual density of the Bi₂Te₃ alloy is measured by using the rule of mixing. Following formulae Equation 5, Equation 6 and Equation 7 were used to find the porosity of the samples:

$$\text{Actual Density} = \frac{\text{Weight in Air}}{\text{Weight in Air} - \text{Weight in Water}} \quad (5)$$

$$\text{Densification (\%)} = \frac{\text{Actual Density}}{\text{Theoretical Density}} \times 100 \quad (6)$$

$$\text{Porosity} = 100 - \text{Densification} \quad (7)$$

3.3.6 Differential scanning calorimeter (DSC)

Differential scanning calorimetry (DSC) was used to examine the thermal properties of the samples. It provides information about the phase changes displayed by the sample, such as a function of temperature. It provides information about the sample melting point (T_{m,p}), enthalpy (ΔH), specific heat (ΔS), glass transition phase (T_g), and the sample crystallinity. The main function of this device is to measure the difference in heat flow as a function of time by comparing it with a reference sample. (Perkin Elmer 8500

DSC) was applied to study the different phase changes based on the temperature and the grain growth of the Bi₂Te₃ sample in order to verify the appropriate temperature for SPS. The test took place between temperature range (30~430) °C at a heating rate of 10°C/min. With one cooling cycle, two separate heating cycles and hold cycles. Table 3 summarizes the experimental condition that took place during the DCS analysis test.

Table 3. Shows the DSC experimental conditions.

Cycle NO.	Cycle Name	Temperature (°C)	Time (min)
1	Heating 1	30~430	1
2	Hold 1	430	370
3	Cooling	430~30	370
4	Heating 2	430	370
5	Hold 2	430	1

3.3.7 Thermoelectric Properties

The alloyed samples prepared by SPS were utilized to test their thermoelectric properties and characterization. Seebeck coefficient (S) and electrical conductivity (σ) were both measured using SBA 458 Nemesis system at temperature (52, 76, 100, 125, and 150 °C) with a heating rate of 25 °C/min. Based on what mentioned in section 3.2.2, after loading the samples inside the system, micro-sized heaters are placed to generate temperature gradient equally in each direction. The resulting voltage is then measured using thermocouples. As for the electrical conductivity (σ) measurements, several current values were tested, and the resulting voltage was obtained. Electrical conductivity (σ) depends several temperature dependant parameters as presented in equation 8.

$$\sigma = \eta e \mu \quad (8)$$

Where (e) is the material charge, (η) is the concentration and (μ) is the mobility of charge carriers. The material electrical conductivity is highly affected when using a nanostructuring approach through the ball milling process and nanocompositing techniques. The ball milling process aids in size reduction of the material grains, as mentioned in section 3.2.1, which in turn increases the mobility of electrons by increasing the number of the grains interface. While the addition of MWCNT through nanocomposite increases the number of charge carriers at the grains boundary results in increasing η of the material.

In order to calculate the Seebeck coefficient (S), a relation between the resulting voltage and the temperature must be calculated equation 9.

$$S = \frac{V_2 - V_1}{T_2 - T_1} = \frac{\Delta V}{\Delta T} \quad (9)$$

To measure the thermal conductivity (k) of the samples, Light Flash Apparatus LFA 467 HyperFlash was used. It considered one of the fastest nondestructive techniques used for determining the thermo-physical properties of the samples. The sample surface is subjected to energy light pulse in short-range, while an infrared x-ray (IR) detector attached at the sample back measures the temperature. Thermal conductivity can be measured using equation 10.

$$K_{Tot.} = K_E + K_L = a\rho C_p \quad (10)$$

Where K_E is the electronic thermal conductivity and K_L is the lattice thermal conductivity, or it can be measured by calculating a is thermal diffusivity, C_p is the specific heat, and ρ

is bulk density. However, the electrical conductivity can be measured using Wiedemann-Franz law equation 11.

$$K_E = \sigma T L \quad (11)$$

Where T is the temperature, σ is the thermal conductivity of the material and L is the Lorentz number ($1.7 \times 10^{-8} \text{ V}^2/\text{K}^2$). The lattice thermal conductivity (K_L) is usually calculated after measuring both K_{Tot} . And K_E . The lattice thermal conductivity is strongly affected by nanocompositing and nanostructuring in which both techniques increase the number of electrons interference between the grain boundaries resulting in an increase in the electrons scattering, electron mobility, and the number of charge carriers.

CHAPTER 4: RESULTS AND DISCUSSION

4.1. Surface morphology and composition

4.1.1. Scanning electron microscopy (SEM) and Energy dispersive X-ray (EDX)

SEM was used to study the elemental distribution and the MWCNT position in the material, as well as the grain distribution. In order to demonstrate the effectiveness of the MWCNT and its role in enhancing the thermoelectric properties of Bi_2Te_3 . A scanning electron microscopy was conducted on the alloyed sample to study the surface morphology of the elements present as well as the exact position of graphene in the material. The SEM image Fig.5 shows the MWCNT; based on the study done in (C.H. Laurent, 2010), the density of CNT was found to be 1.1 with an average diameter of 12.6nm. Refer to appendix for the density of CNTs measured based on the outer diameter for a different number of walls. Figure 6 shows the a) Bi_2Te_3 and b) MWCNT/ Bi_2Te_3 . The MWCNT could not be seen clearly in the SEM image despite been reported in the EDX Figure.5 this might be due to the longer milling process of 16 hours that leads the MWCNT to be shielded by Bi_2Te_3 during the process.

The Energy Dispersive X-ray (EDX) mapping test was conducted to confirm the presence of MWCNT in the Bi_2Te_3 system. Based on Figure 7-B the presence of MWCNT was confirmed compared with the base material (Bi_2Te_3) in figure 7-A.

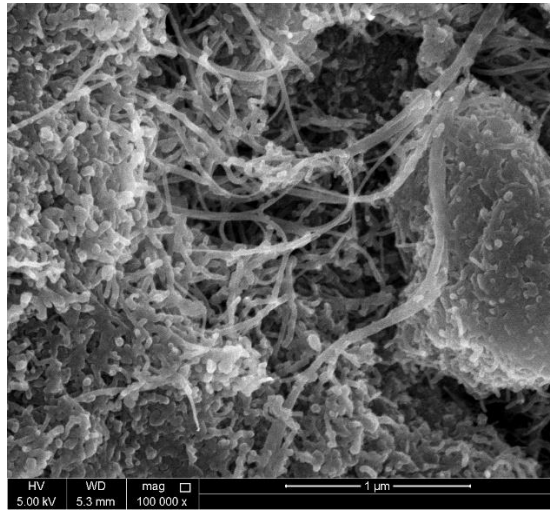


Figure 5. shows the MWCNT used to dope Bi_2Te_3 base.

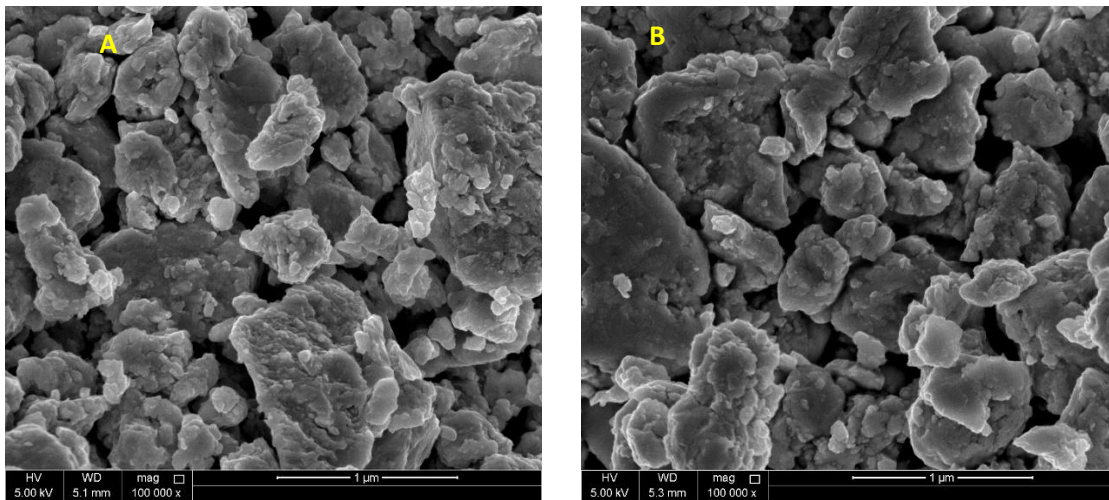


Figure 6. SEM images shows the composites alloys a) Bi_2Te_3 , b) 1% MWCNT/ Bi_2Te_3 .

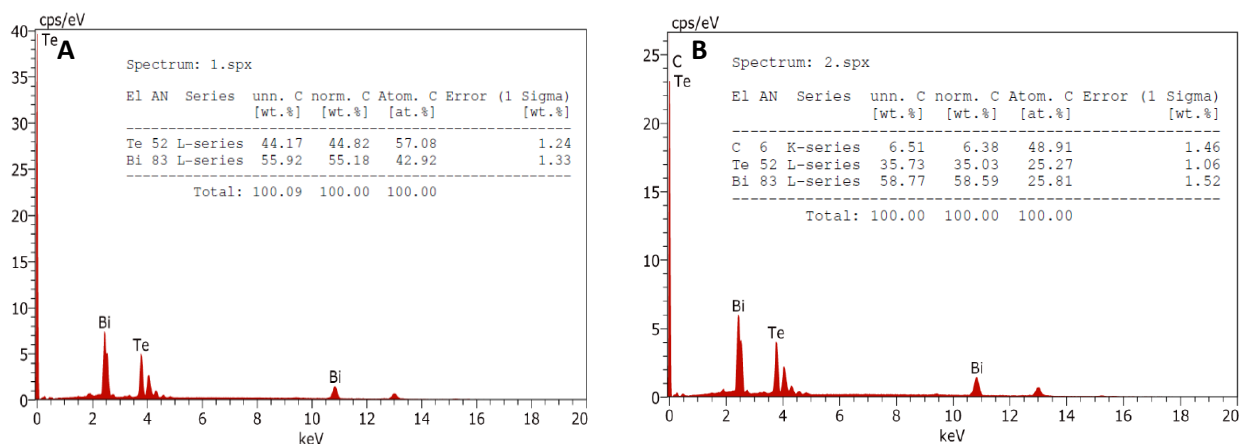


Figure 7. Shows the EDX analysis of the composites alloys a) Bi_2Te_3 , b) 1% MWCNT/ Bi_2Te_3 .

4.1.2. X-ray diffraction (XRD)

Figure 8 represents the XR-diffraction results performed on Bi_2Te_3 and Bi_2Te_3 -MWCNT prepared by mechanical ball milling for 16 hours, based on X-ray diffraction a very clear diffraction peaks are reported, the peaks did not shift as an effect of the long milling process and no broadening of the peaks took place. The reported peaks are matching the standard peaks of rhombohedral Bi_2Te_3 (JCPDS No. 48-1224). The progression of the peaks shown in Figure 8 indicates a comparable behavior for the base material Bi_2Te_3 , since no shift or additional peaks were observed. MWCNT peaks cannot be detected due to lower (1% wt%) percentage content, as reported in other research studies (B. Khasimsaheb, 2017). Further analyzes and calculations were done to assess the grain size and the strain of the prepared nanocomposites using the Averbach method by calculating the Full-Width Half Maximum (FWHM) of each peaks using equation 5 as explained in chapter 3 section 3.3.3. The generated slope and the intercept were used to

evaluate the grain size and strain. Figure 9 represents a different variation of grain size and strain with different MWCNT content for all samples.

Based on Table.4, the major peaks presented in the XRD were used to calculate the grain size in order to determine Hall–Petch contribution of MWCNT to the Bi_2Te_3 hardness using Equation 5, as well as the amount of strain and the SPD the system was subjected during the milling process. The average grain size of Bi_2Te_3 was found to be 13 nm, and the lattice strain during the milling process was found to be 0.21 based on the Averbach equation.

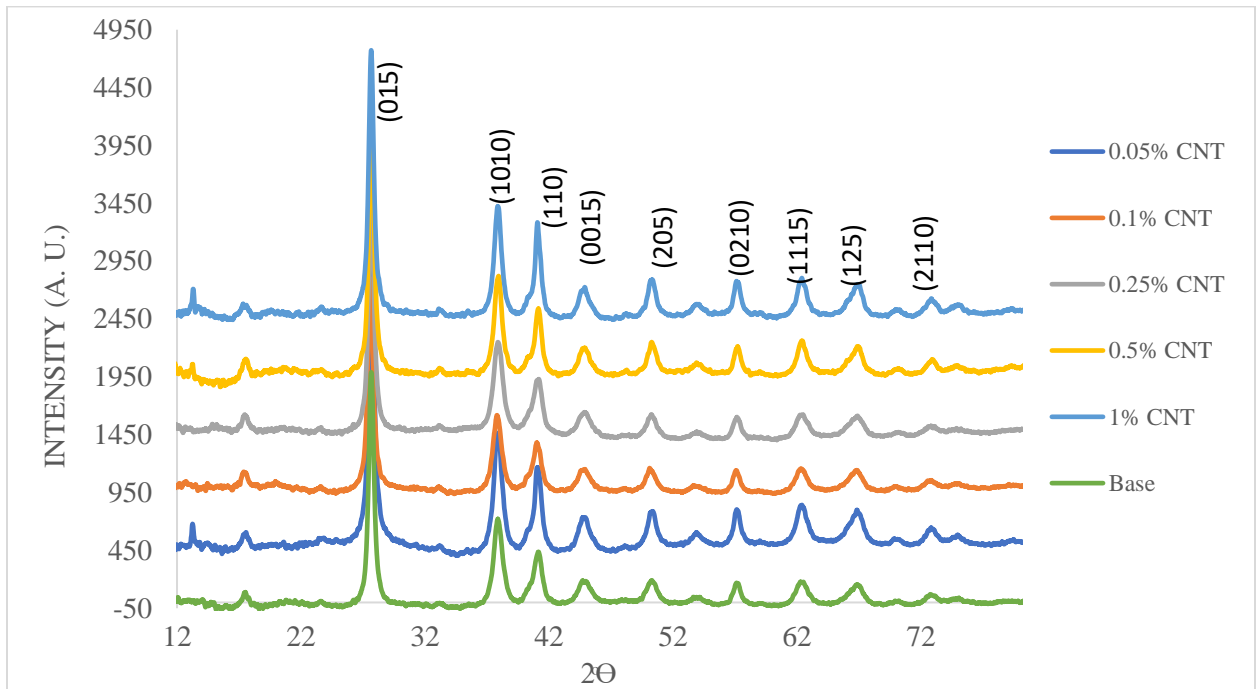


Figure 8. XRD analysis of as prepared Bi_2Te_3 , Bi_2Te_3 –0.05% MWCN, Bi_2Te_3 – 0.1% MWCNT, Bi_2Te_3 – 0.25% MWCNT, Bi_2Te_3 – 0.5% MWCNT and Bi_2Te_3 – 1%MWCNT.

Table 4. Shows the grain size and the strain of Bi₂Te₃ and the dropped MWCNT/Bi₂Te₃.

Averbach Liner Fit		
Composition	Grain Size (nm)	Strain
Bi₂Te₃	11.846	0.179
0.05 CNT/Bi₂Te₃	12.419	0.200
0.1 CNT/Bi₂Te₃	12.419	0.155
0.25 CNT/Bi₂Te₃	14.144	0.299
0.5 CNT/Bi₂Te₃	14.393	0.190
1 CNT/Bi₂Te₃	15.098	0.200
AVG	13.044	0.205

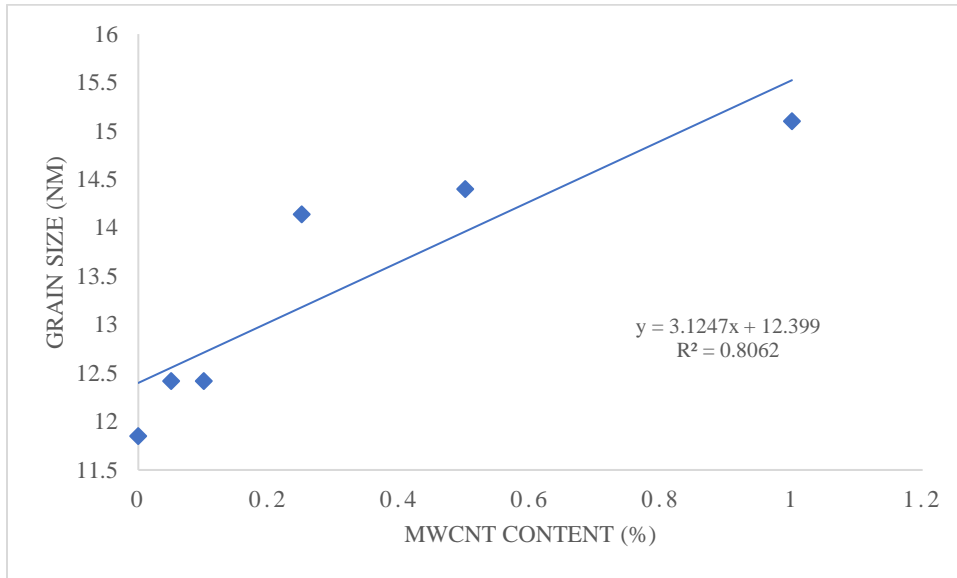


Figure 9. Shows the liner fit of Averbach method to calculate the Grain size and Lattice strain of Bi₂Te₃ as function of different MWCNT content.

4.1.3. Transmission electron microscopy (TEM)

For further confirmation regarding the structural and the grain size of the nanocomposites obtained from XRD. TEM was used on base material Bi₂Te₃ and MWCNT- Bi₂Te₃ nanocomposite that was prepared with different MWCNT content.

Figure 10-a and Figure 10-b present the bright and dark-field TEM image of MWCNT- Bi_2Te_3 , respectively. It can be concluded from the bright-field images that the nanograins possess high angle grain boundaries as the scale is 200 nm. The dark field images were utilized to estimate the average grain size. Based on figure 11, the average grain size distribution was found to be between 6 ~10 nm, with a lower limit of ~1 nm and upper limit distribution of 20 nm. The obtained values are relatively consistent with the grain size value acquired from the XRD analysis and the Averbach equation. The slight differences in size calculation may possibly be due to the Averbach method fitting or the unclear selection of the grains in the TEM images. Based on these results nanostructuring of Bi_2Te_3 using high energy ball mill is a successful fabrication method.

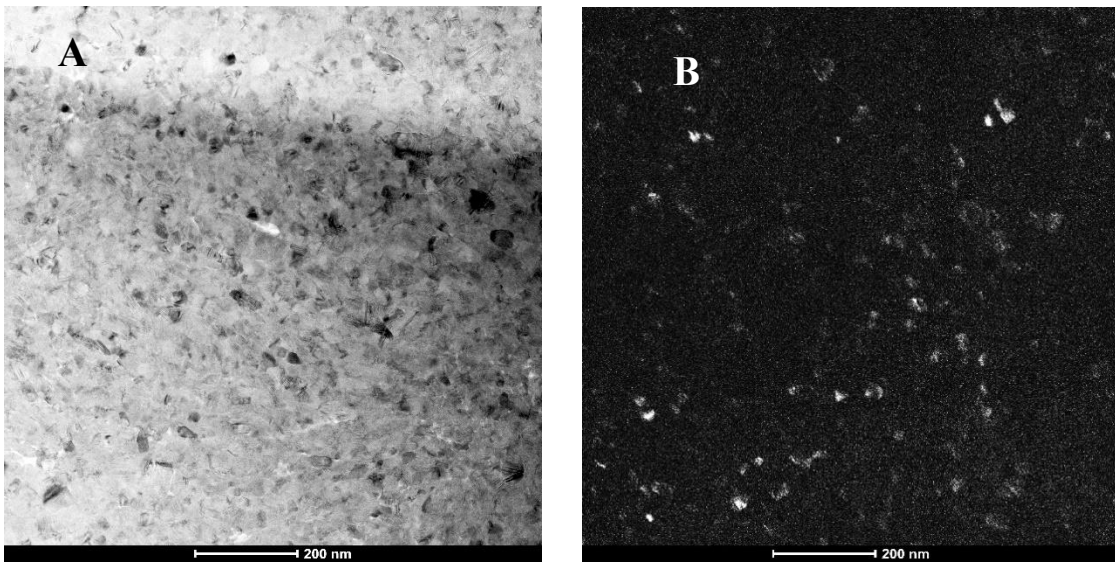


Figure 10. shows a) bright-field TEM image, b) dark-field TEM image of MWCNT- Bi_2Te_3 .

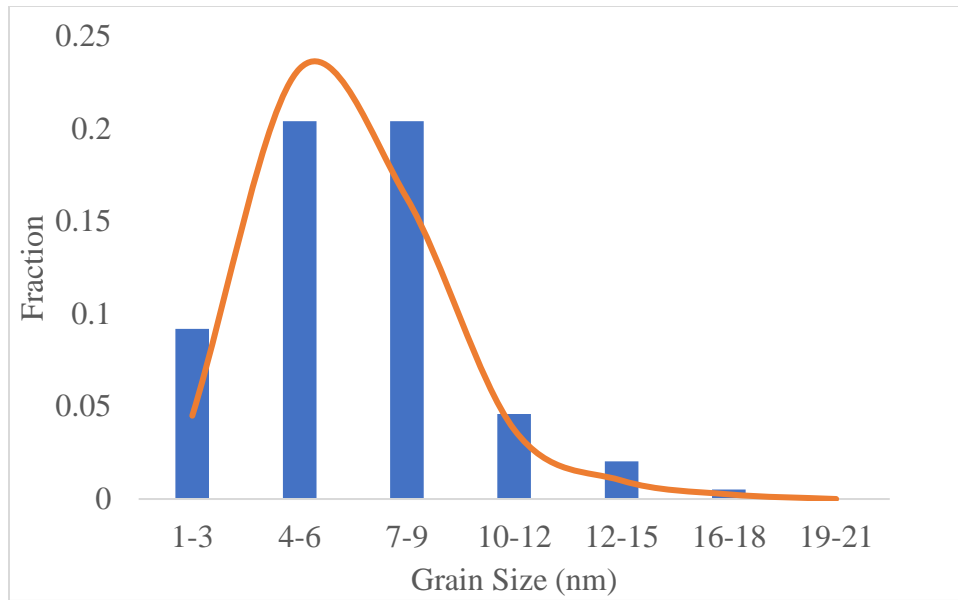


Figure 11. Shows the Grain size distribution of MWCNT-Bi₂Te₃ and the Lorentz fitting of the fraction distribution.

4.2. Mechanical and physical properties

4.2.1. Vicker microhardness

The mechanical properties of the material are very critical since it contributes to the material performance and resistance to plastic deformation during the exposure to high loads and stresses. Vickers microhardness analysis test was conducted on Bi₂Te₃ and MWCNT- Bi₂Te₃ nanocomposites samples. The hardness values obtained with respect to MWCNT content are presented in Figure 12. From the figure, it can be seen that the material hardness increases gradually with increasing MWCNT content. Which is an expected outcome based on what is reported in (R. Christopher and others, 2014) due to the nature of MWCNT. The hardness values increase as the MWCNT content increase in

Table 6. This may be a result of the increasing weight fraction of hard and brittle phase, which results in increasing dislocation density, which in turn will promote the enhancement of mechanical property.

Table.5 shows the microhardness values obtained from the analysis machine in Hv, while Table 6 shows the average hardness values of each sample after the conversion to MPa and GPa. Based on table.5, the microhardness analysis of Bi_2Te_3 and the doped Bi_2Te_3 with MWCNT were found to be increasing as the volume percentage content of MWCNT is increasing. The base material (Bi_2Te_3) hardness was found to be ~148 Hv, while at 1% MWCNT composite, it was found to be ~200 Hv. Table.6 shows the microhardness analysis of Bi_2Te_3 and the doped Bi_2Te_3 with MWCNT were found to be increasing as the weight percentage content of MWCNT is increasing. The base material (Bi_2Te_3) hardness was found to be ~1.45 GPa, while at 1% MWCNT composite it was found to be ~1.95 GPa. The hardness of the Bi_2Te_3 is less than the reinforced Bi_2Te_3 with MWCNT; the lower value can be justified by the empty spaces between the grain boundaries and the stress sliding that take place at such small size. The increase in hardness values can be attributed to the strong nanostructuring and the nature of MWCNT. MWCNT at the grain boundaries acts as a barrier preventing any dislocation motion, slip planes, or defects during the exposure of stress. It considered one of the most used strengthening mechanisms in nanostructuring.

Table 5. Shows the microhardness values (Hv) based on the MWCNT content.

CNT(%)	0%	0.05%	0.10%	0.25%	0.50%	1%
No.1	134.54	150.93	169.38	168.1	186.49	204.46
No.2	145.43	166.26	155.53	159.19	169.2	188.69
No.3	160.14	165.72	150.48	153.23	181.32	192.88
No.4	157.47	146.08	152.27	155.31	171.9	190.62
No.5	152.29	152.50	162.59	151.17	163.41	212.53
No.6	137.44	141.84	151.12	149.36	177.28	201.29
AVG	147.89	153.89	156.90	156.06	174.93	198.41

Table 6. Shows the microhardness values (Hv, MPa and GPa) based on the MWCNT content.

CNT%	Hv	Mpa	Gpa
0	147.89	1450	1.45
0.05	153.89	1509	1.51
0.1	156.9	1539	1.54
0.25	156.06	1530	1.53
0.5	174.93	1716	1.72
1	198.41	1946	1.95

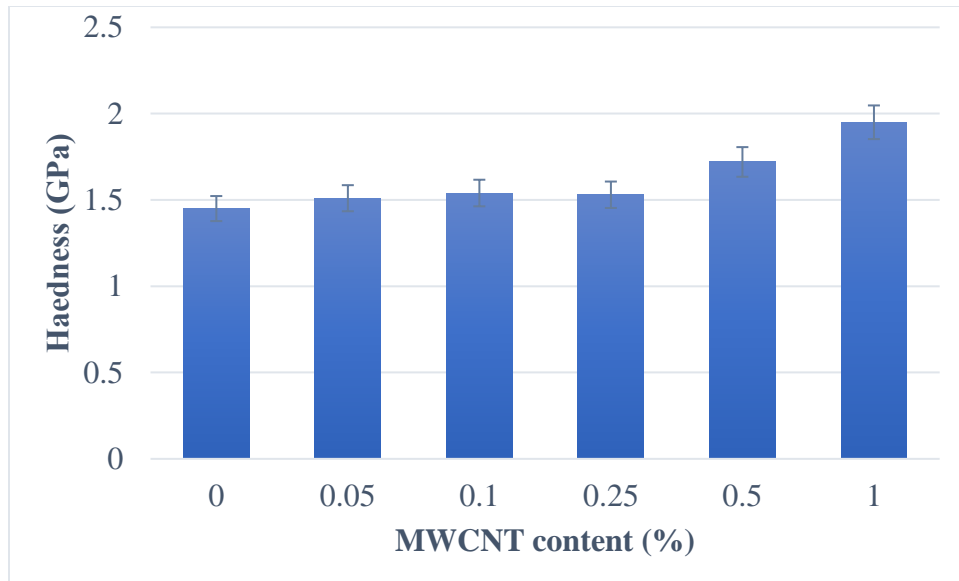


Figure 12. Shows the microhardness values (GPa) based on the MWCNT content.

4.3. Thermal and electrical properties

4.3.1. Differential scanning calorimeter (DSC)

Based on Figure 13 and figure 14, the data obtained from the DSC shows that there is some consistency between the base material and the doped alloys, in which the temperature range of the grain growth (exothermic) is between 370~400°C figure 13. The melting points (endothermic) of the first heating cycle of all systems were around ~416 °C and the second melting temperature (endothermic) of the second cycle was around ~417 °C, Figure 14. As for the enthalpy of mixing, it range from 1.6 J/g to 4.6 J/g. Table 7 shows the data obtained from the DCS test.

Table 7. Shows the DSC results of the base on doped Bi₂Te₃ with MWCNT.

Samples No.	Grain growth Temp. (°C)	First T _{mp} (°C)	Second T _{mp} (°C)	ΔH (J/g)
Base (Bi ₂ Te ₃)	370~400	416.39	417.36	3.315
Bi ₂ Te ₃ -0.05%SWCNT	374.5~400	415.88	417.68	1.666
Bi ₂ Te ₃ -0.1%SWCNT	374~400	416.37	417.67	4.469
Bi ₂ Te ₃ -0.25%SWCNT	375.6~400	416.38	417.66	4.622
Bi ₂ Te ₃ -0.5%SWCNT	374~400	416.69	416.88	3.654
Bi ₂ Te ₃ -1%SWCNT	375.6~400	415.88	417.84	3.251

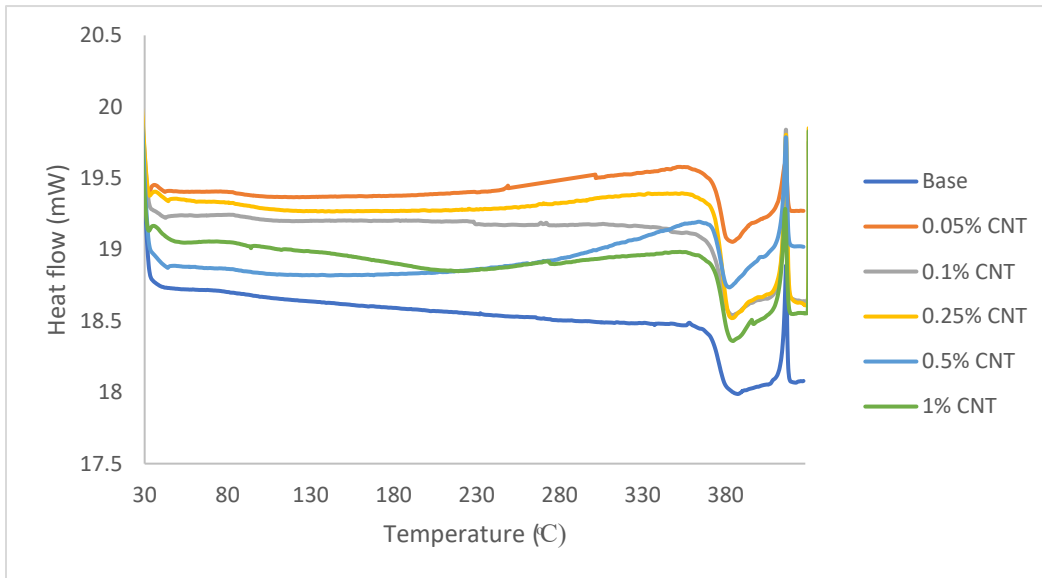


Figure 13. DSC curve of the 1st heat analysis of bismuth telluride and the doped alloy.

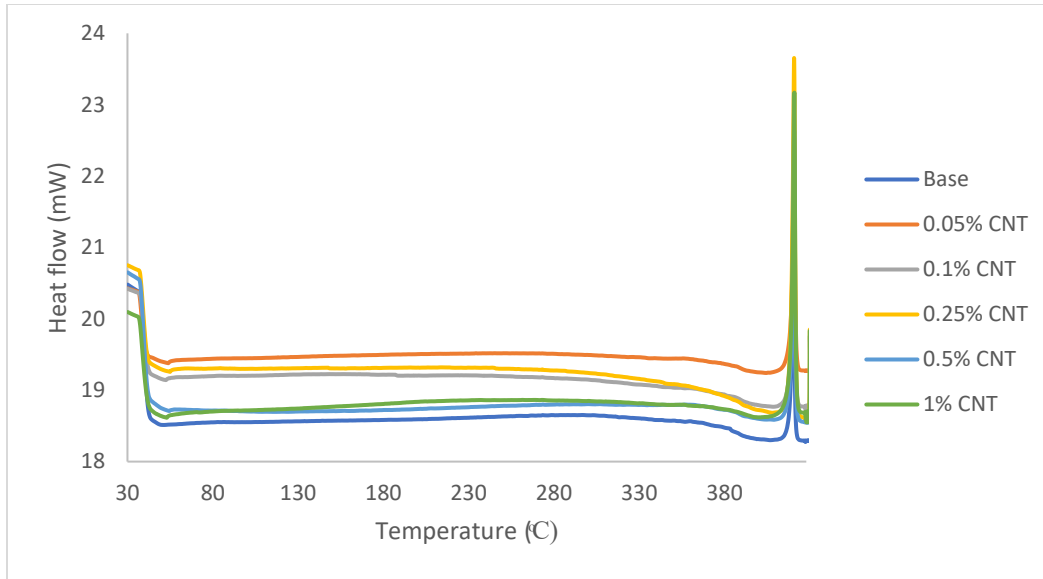


Figure 14. DSC curve of the 2nd heat analysis of bismuth telluride and the doped alloy.

4.4. Thermoelectric measurements

The Seebeck coefficient (S), Electrical resistivity (ρ), Thermal conductivity (k), and the Power factor (PF) are all temperature dependence properties. Figure 15 presents the above results of both Bi_2Te_3 and MWCNT/ Bi_2Te_3 nanocomposite, prepared at 16 hrs, and consolidated by spark plasma sintering technique (SPS).

4.4.1 Thermoelectric properties of Bi_2Te_3 and MWCNT/ Bi_2Te_3

Figure 15.a shows the variation of electrical conductivity as a function of the temperature of both Bi_2Te_3 and MWCNT/ Bi_2Te_3 samples. It can be seen that there is a decrease in electrical conductivity as the temperature is increased. It can be due to the increase in charge carrier scattering as the temperature increases. As well as the high

density of MWCNT accumulated at the grain boundaries acting as charge barriers. A behavior is known for degenerate semiconductors/metal-like transport.

Figure 15.b presents the change in the Seebeck coefficient with the temperature change. The decrease in the Seebeck coefficient with the dispersion of MWCNTs in the Bi_2Te_3 system can be due to the reduction in the charge carrier mobility due to the smaller grain size of the MWCNT. The thermally excited minority carriers have a greater effect at higher temperatures terminating the effect of Seebeck. The thermally excited electron-hole pair effect in the Bi_2Te_3 system was lower than the doped MWCNT/ Bi_2Te_3 due to the larger charge carrier concentration. The maximum Seebeck effect of MWCNT/ Bi_2Te_3 composite was obtained at temperature 77°C in the 1%MWCNT/ Bi_2Te_3 system. It is expected that the slower reduction in Seebeck at higher temperatures leads to relatively high ZT values.

Figure 15.c represents the thermal conductivity of Bi_2Te_3 and MWCNT/ Bi_2Te_3 . The addition of MWCNT has significantly affected the thermal conductivity of the samples. The decreased in thermal conductivity can be due to the additional scattering between the Bi_2Te_3 and MWCNT phase boundaries created as a result of increasing the temperature.

Figure 15.d shows the power factor as a function of the temperature of the both Bi_2Te_3 and MWCNT/ Bi_2Te_3 . The addition of MWCNT offers a better power factor than pure Bi_2Te_3 . At 150°C for the Bi_2Te_3 compared to MWCNT/ Bi_2Te_3 from $104\ \mu\text{W}/\text{mK}^2$ to $135\ \mu\text{W}/\text{mK}^2$ respectively.

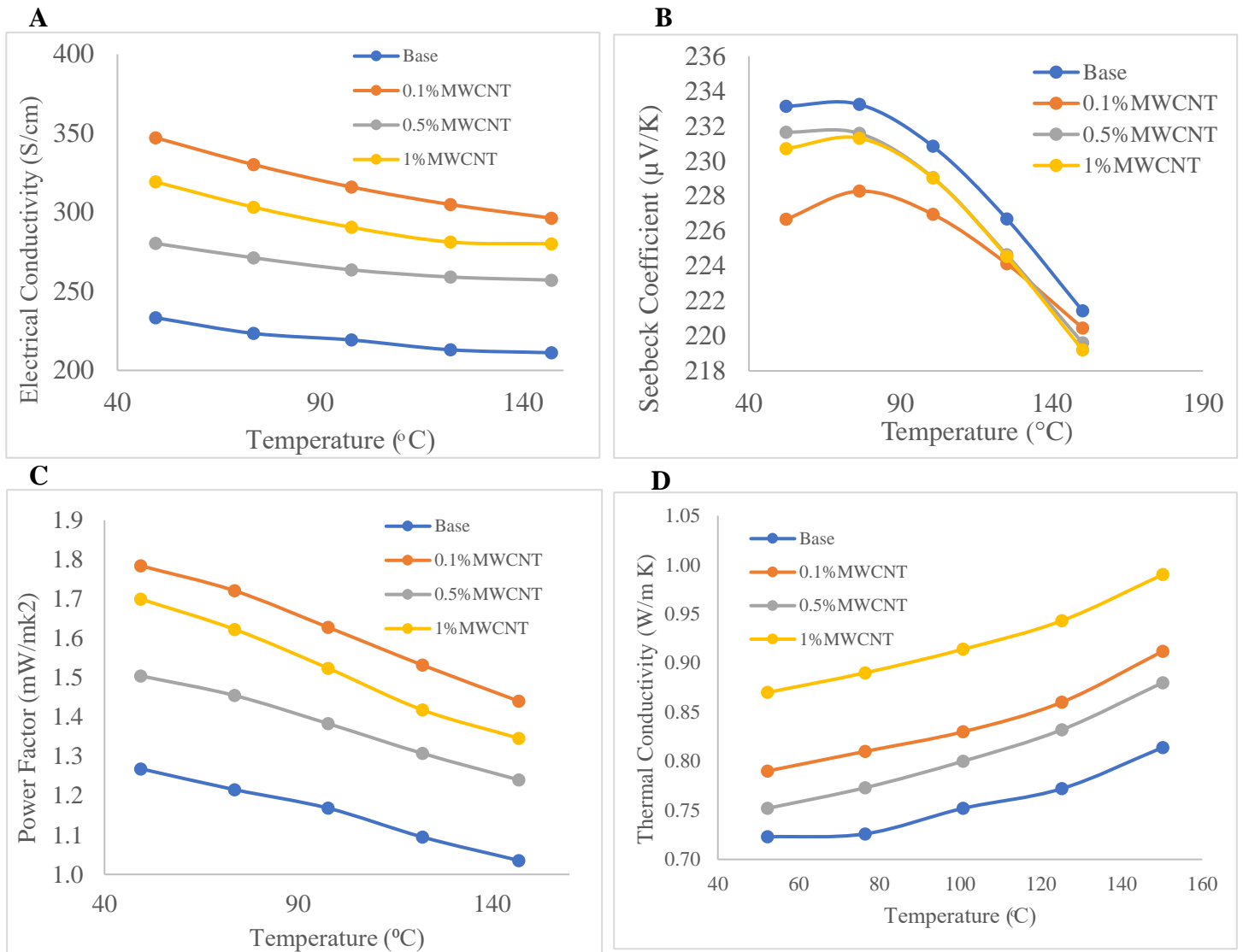


Figure 15. Shows the Bi_2Te_3 and $\text{MWCNT}/\text{Bi}_2\text{Te}_3$ prepared by ball milling and SPS. a)Electrical conductivity, b)Seebeck Coefficient, c)Thermalconductivity and d)Power Factor.

4.4.2. The figure of merit (ZT)

Figure 16 presents the figure of merit (ZT) values for the prepared nanostructured Bi_2Te_3 and MWCNT/ Bi_2Te_3 nanocomposite. As shown in Figure 16, the addition of MWCNT increased the ZT value from 0.48 to maximum ZT value to 0.61 at 50°C, while in the research conducted by (K. T. Kim, S. Y. Choi and others, 2013) the ZT values of Bi_2Te_3 and MWCNT/ Bi_2Te_3 at the same temperature were found to be 0.28 and 0.48 respectively. At 150°C, the ZT value was measured to be 0.35 and 0.43 for Bi_2Te_3 and MWCNT/ Bi_2Te_3 respectively. The noticeable enhancement in the ZT value is a result of a higher power factor due to the addition of MWCNT. The attained results from this work can be further improved by doping.

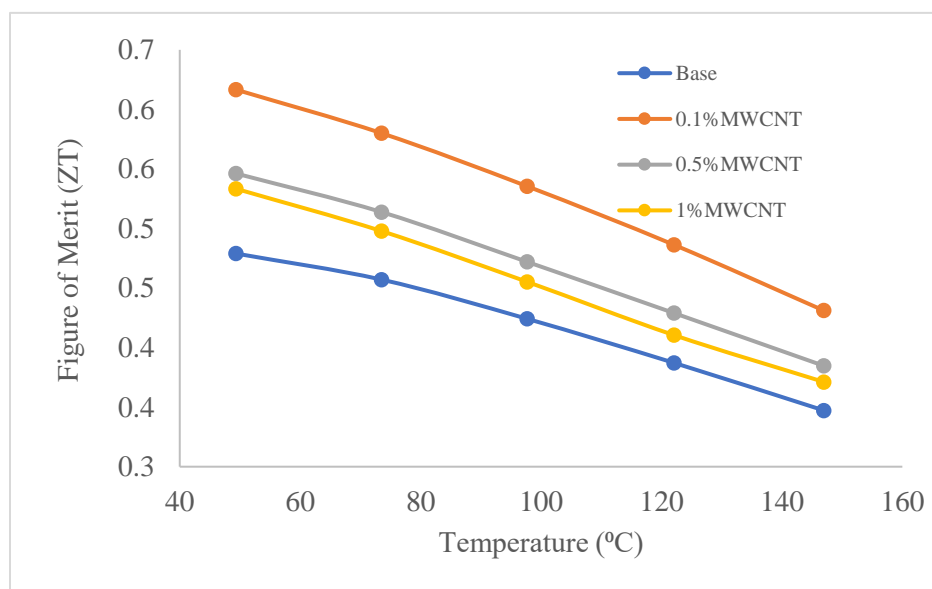


Figure 16. Comparison between the figure of merit (ZT) of Bi_2Te_3 and MWCNT/ Bi_2Te_3 nanocomposite.

CHAPTER 5: CONCLUSION

In summary, nanocrystalline Bi_2Te_3 and MWCNT/ Bi_2Te_3 composites were effectively prepared by high energy ball milling under inert atmosphere then the manufactured powder was consolidated using SPS technique. The mechanical, structural, and thermal properties of the samples were assessed, and the material thermoelectric properties were measured at five different temperatures. Several findings were obtained from this study, and the following paragraph summarizes the main major findings in this research.

The average grain size of both nanocomposites (Bi_2Te_3 and MWCNT/ Bi_2Te_3) was around (6~10 nm). The addition of MWCNT into the Bi_2Te_3 structure showed an enhancement in its mechanical property, with an increase in the microhardness value from ~1.45 GPa to ~1.95 GPa as the MWCNT content increases. The addition of MWCNT to Bi_2Te_3 increased its charge density transfer, leading to an increase in the electrical conductivity of the material. As well as lowering the thermal conductivity of the system by producing extra phonon scattering sites. The alloying process contributes in more charge carriers scattering, which in turn increases the power factor from $104 \mu\text{W}/\text{mK}^2$ to $135 \mu\text{W}/\text{mK}^2$ at 150°C . The ZT values of pure Bi_2Te_3 was also increased from 0.35 to maximum ZT value to 0.43 at 150°C . It is assumed that MWCNT is primarily present at the grain boundaries of Bi_2Te_3 .

CHAPTER 6: REFERENCES

- [1] B. Khasimsaheb, Niraj Kumar Singh, Sivaiah Bathula, Bhasker Gahtori, D. Haranath, S. Neeleshwar. The effect of carbon nanotubes (CNT) on thermoelectric properties of lead telluride (PbTe) nanocubes, *Current Applied Physics*, (2017), 17, 306-313. Doi.org/10.1016/j.cap.2016.05.026
- [2] C. Yu, Y. S. Kim, D. Kim, J. C. Grunlan. Thermoelectric behavior of segregated-network polymer nanocomposites. *Nano Lett* (2008, 8:4428–32.
- [3] C. Gayner and K. K. Kar, “Recent advances in thermoelectric materials,” *Prog. Mater. Sci.*, (2016), vol. 83, pp. 330–382.
- [4] C. Suryanarayana, “Synthesis of nanocomposites by mechanical alloying,” *J. Alloys Compd.*, vol. 509, no. SUPPL. 1, pp. S229–S234, 2011.
- [5] C.H. Laurent, Christophe and Flahaut, Emmanuel and A. Peigney, Alain. The weight and density of carbon nanotubes versus the number of walls and diameter. *Carbon*, (2010), vol. 48 (n° 10). pp. 2994-2996. ISS N 0008-6223
DOI:10.1016/j.carbon.2010.04.010
- [6] D. H. Park, M. Y. Kim, T.-S. Oh, Thermoelectric energy-conversion characteristics of n-type Bi₂(Te, Se)₃ nanocomposites processed with carbon nanotube dispersion, *Curr. Appl. Phys.*, (2011), 11: 41-45.
- [7] D. Suh, S. Lee, H. Mun, S. H. Park, K. H. Lee, S. W. Kim, J. Y. Choi and S. Baik, Enhanced thermoelectric performance of Bi_{0.5}Sb_{1.5}Te₃-expanded graphene composites by simultaneous modulation of electronic and thermal carrier transport, *Nano Energy*, (2015) 13, 67–76

[8] F.J. Disalro . Thermoelectric cooling and power generation, Science (1999), 285:5428,703–706.

DOI: 10.1126/science.285.5428.703

[9] F. Ren, H. Wang, P. A. Menchhofer, J. O. Kiggans. Thermoelectric and mechanical properties of multi-walled carbon nanotube doped $\text{Bi}_{0.4}\text{Sb}_{1.6}\text{Te}_3$ thermoelectric material. App. Phys. Lett. (2013), 103

[10] L. D. Zhao, B. -P. Zhang, J. -F. Li, H. L. Zhang, W. S. Liu ‘Enhanced thermoelectric and mechanical properties in textured n-type Bi_2Te_3 prepared by spark plasma sintering’, (2008), 10, 651-658.

[11] J. Sharp, J. Bierschenk, and H. B. Lion, Overview of solid-state thermoelectric refrigerators and possible applications to on-chip thermal management Jr., Proc. IEEE. (2006), 94(8), 1602

[12] J.B. Wachtman, W. R. CANNON, M. J. MATTHEWSON. Mechanical Properties of Ceramics, Wiley and sons Interscience publication, Rutgers University, New York, NY (1996).

[13] K. T. Kim, S. Y. Choi, E. H. Shin, K. S. Moon, H. Y. Koo, G. G. Lee, et al. The influence of CNTs on the thermoelectric properties of a CNT/ Bi_2Te_3 composite. Carbon (2013), 52:541-549.

[14] K. Agarwal, V. Kaushik, D. Varandani, A. Dhar, & B. R. Mehta. Nanoscale thermoelectric properties of Bi_2Te_3 – Graphene nanocomposites: Conducting atomic

force, scanning thermal and kelvin probe microscopy studies. *Journal of Alloys & Compounds*, (2016), 681, 394-401.

Doi:10.1016/j.jallcom.2016.04.161.

[15] L. Cheng, Z.-G. Chen, L. Yang, G. Han, H.-Y. Xu, G.J. Snyder, G. Q. Lu, J. Zou, T-shaped Bi_2Te_3 -Te heteronanojunctions: epitaxial growth, structural modeling, and thermoelectric properties, *J. Phys. Chem. C* 117 (2013), 12458–12464.

[16] M. G. Kanatzidis Nanostructured Thermoelectrics: The New Paradigm?, *Chemistry of Materials* (2010) 22 (3), 648-659. DOI: 10.1021/cm902195j

[17] M. Hong, Z. G. Chen and J. Zou, Fundamental and Progress of Bi_2Te_3 Thermoelectric Materials, *Chinese Physical Society* (2018), 27, 1-4.

DOI: 10.1088/1674-1056/27/4/048403

[18] N. Gothard, T. M. Tritt, J. Spowart. Figure of merit enhancement in bismuth telluride alloys via fullerene-assisted microstructural refinement. *J Appl Phys* (2011), 110:023706

[19] Q, Lognoné, & F. Gascoin. “On the effect of carbon nanotubes on the thermoelectric properties of n- $\text{Bi}_2\text{Te}_{2.4}\text{Se}_{0.6}$ made by mechanical alloying”. *Journal of Alloys & Compounds* (2015), 635, 107-111.

Doi:10.1016/j.jallcom.2015.02.055.

[20] R. Christopher, Bradbury, Jaana-Kateriina Gomon, Lauri Kollo, Hansang Kwon, Marc Leparoux, Hardness of Multi Wall Carbon Nanotubes reinforced aluminium

matrix composites, *Journal of Alloys and Compounds*, (2014), Volume 585, Pages 362-367, ISSN 0925-8388.

[21] T. M. Tritt and M. A. Subramanian, *Thermoelectric Materials, Phenomena, and Applications: A Bird's Eye View*. *MRS Bulletin* (2006), 31, 188-197.

[22] T. H. Nguyen, J. Enju and T. Ono, Enhancement of Thermoelectric Properties of Bismuth Telluride Composite with Gold Nano-Particles Inclusions Using Electrochemical Co-Deposition, *Journal of The Electrochemical Society*, 166 (12) D508-D513 (2019)

DOI: 10.1149/2.1011912jes

[23] W. Xie, X. Tang, Y. Yan, Q. Zhang, T. M. Tritt. Unique nanostructures and enhanced thermoelectric performance of melt-spun BiSbTe alloys. *Appl Phys Lett* (2009), 94:102111.

[24] W. Kim, J. Zide, A. Gossard, D. Klenov, S. Stemmer, A. Shakouri, et al. Thermal conductivity reduction and thermoelectric figure of merit increase by embedding nanoparticles in crystalline semiconductors. *Phys Rev Lett* (2006), 96:045901.

[25] Y. Zhang, X. L. Wang, W. K. Yeoh, R. K. Zheng and C. Zhang. Electrical and thermoelectric properties of single-wall carbon nanotube doped Bi₂Te₃. *App. Phy. Lett.* (2012). Vol. 102. Iss.1 10.1063

Doi.org/10.1063/1.4775732

[26] Z. G. Chen, G. Han, L. Yang, L. Cheng and J. Zou, Nanostructured thermoelectric materials: Current research and future challenge, *Progress in Natural Science: Materials International* (2012), 22(6):535–549